10-10-2005

# Characterization of Surface Roughness Effects on Pressure Drop in Single-Phase Flow in Minichannels

Satish G. Kandlikar

Derek Schmitt
*Rochester Institute of Technology*

Andres L. Carrano
*Rochester Institute of Technology*

James B. Taylor
*Rochester Institute of Technology*



Recommended Citation
S. G. Kandlikar, D. Schmitt, A. L. Carrano, and J. B. Taylor, "Characterization of surface roughness effects on pressure drop in single-phase flow in minichannels," Physics of Fluids https://doi.org/10.1063/1.1896985 17, 10 (2005).

# Characterization of surface roughness effects on pressure drop in single-phase flow in minichannels

Satish G. Kandlikar[8)] and Derek Schmitt

*Department of Mechanical Engineering, Rochester Institute of Technology, Rochester, New York 14618*

Andres L. Carrano and James B. Taylor

*Industrial and Systems Engineering, Rochester Institute of Technology, Rochester New York 14618*

Roughness features on the walls of a channel wall affect the pressure drop of a fluid flowing through that channel. This roughness effect can be described by (i) flow area constriction and (ii) increase in the wall shear stress. Replotting the Moody's friction factor chart with the constricted flow diameter results in a simplified plot and yields a single asymptotic value of friction factor for relative roughness values of $e/D > 0.03$ in the fully developed turbulent region. After reviewing the literature, three new roughness parameters are proposed (maximum profile peak height $R_p$, mean spacing of profile irregularities Rsm, and floor distance to mean line $F_1$,). Three additional parameters are presented to consider the localized hydraulic diameter variation (maximum, minimum, and average) in future work. The roughness $e$ is then defined as $R_p + F_p$,. This definition yields the same value of roughness as obtained from the sand-grain roughness [H. Darcy, *Recherches Experimentales Relatives au Mouvement de L'Eau dans les Tuyaux* (Mallet-Bachelier, Paris, France, 1857); J. T. Fanning, A *Practical Treatise on Hydraulic and Water Supply Engineering* (Van Nostrand, New York, 1877, revised ed. 1886); J. Nikuradse, "Laws of flow in rough pipes" [ "Stromungsgesetze in Rauen Rohren," VDI-Forschungsheft 361 (1933)]; Beilage cu "Forschung auf dens Gebiete des Ingenieurwesens," Ausgahe B Band 4. English translation NACA Tech. Mem. 1292 (1937)]. Specific experiments are conducted using parallel sawtooth ridge elements, placed normal to the flow direction, in aligned and offset configurations in a 10.03 mm wide rectangular channel with variable gap (resulting hydraulic diameters of 325 um-1819 um with Reynolds numbers ranging from 200 to 7200 for air and 200 to 5700 for water). The use of constricted flow diameter extends the applicability of the laminar friction factor equations to relative roughness values (sawtooth height) up to 14%. In the turbulent region, the aligned and offset roughness arrangements yield different results indicating a need to further characterize the surface features. The laminar to turbulent transition is also seen to occur at lower Reynolds numbers with an increase in the relative roughness.

## I. INTRODUCTION

The effects of surface roughness on pressure drop in circular tubes and rectangular channels have been studied extensively in literature. As early as in the nineteenth century, Darcy' conducted careful pressure drop experiments on pipes of different materials and roughnesses, and introduced the concept of relative roughness. He also established that the flow depended on the pipe roughness, diameter, and slope. Fanning[2] later proposed a correlation for the pressure drop as a function of surface roughness. The pioneering work of quantifying the effect of surface roughness on pressure drop was led by Nikuradse,[3] who established the sand-grain roughness *e*, equivalent to the diameter of the sand particles used in his experiments. as a major parameter affecting the friction factor during laminar and turbulent flows. To create the roughness on the inside walls of the pipes, he first sifted sand grains so that the grains were of uniform size. He the used Japanese lacquer to stick the sand grains to the walls c the pipe. Experimental data were obtained for water flowing, in pipes of six different relative roughness surfaces with R ranging from 600 to $10^6$. The dimensions of the inner diameter *Dt* of the test pipes were 25, 50, and 100 mm. His wad helped in establishing the effect of relative roughness *E/dj* on the flow characteristics. It should be noted that the pip diameter used in his work was the base diameter of the pip( before the sand grains were applied.

Colebrook" later published his findings on the variation in surface roughness and its effect on pressure drop. Cole. brook's experiments included sixteen spun concrete-lined pipes and six spun bitumastic-lined pipes ranging in diameter from 101.6 mm (4 in.) to 1524 min (60 in.). Average rough. ness values ranged from 0.043 18 mm to 0.254 mm. Also tested was the 5486 mm (216 in.) diameter Ontario tunnel. which was a concrete tunnel made from steel oil forms. When the concrete was set and the forms were removed, *the* walls of the tunnel were rubbed down with carborundum brick to remove any excess protrusions. These pipes were

Telephone: 585-475-6728. Electronic mail: sgkeme@rit.edu
[E]lectronic mail: schmittdjg@aol.com
[C]) Telephone: 585-475-6062. Electronic mail: alceie@rit.edu '"
Telephone: 585-475-6185.
Electronic mail: jbteie@rit.edu

tested with water flow in the transition and fully turbulent regions. It was determined that the friction factor decreases as the velocity increases. Once the velocity profile reaches the fully developed profile described by the square law, the friction factor remains constant for all higher velocities.

Moody later characterized the Darcy friction factor Fdarcy as a function of the Reynolds number and relative roughness e/Dt. The Moody diagram was established through Colebrook's work, and it provided engineers with a convenient method of determining the pressure drop as a function of the relative roughness of the pipe surface. The sand-grain diameters in Nikuradse's' experiments were used for roughness s. The average roughness value Ra, obtained from surface profile measurements were later employed while using the Moody diagram. The outlined method of determining pressure drop loses its integrity for higher relative roughness values beyond 5%. Although the current relative roughness values used in the plots go only as high as 5%, higher values *are* expected with flows in small diameter channels encountered in a number of applications, such as high heat flux cooling, microfluidics, and biological applications.

Webb *et al.*[6] studied the flow separation during fluid flow over repeating roughness elements. Flow separated from the wall following the roughness elements and then reattached at a distance of six to eight times the height of the element. For surface roughness resulting from a manufacturing process, such as machining or surface treatment, the roughness elements are similar in nature and are closely spaced. The flow encounters the leading element and skims over a pocket of circulating fluid before passing over the next element.

In the present paper, the constriction effect is used to modify the Moody diagram by replacing the root diameter with the constricted flow diameter for circular pipes in both laminar and turbulent regions. Further, to identify the effects of higher relative roughness on laminar and turbulent friction factors, systematic experiments are conducted using air and water as working fluids in rectangular minichannels. The dependence of the laminar-to-turbulent transition on the relative roughness is investigated in an effort to understand the reasons for early transitions (for Re < 2100) reported in literature, for example, Mala and Li' with Dh from 50 to 254 Am, and Wang and Peng[8] with 300-750 ,um. The surface feature effect is also studied by using aligned and ffset sawtooth profiles machined on two 10.03 mm wide walls of the flow channel separated by a small gap. The gap

varied to change the hydraulic diameter of the channel. ince the roughness features cannot be accurately described the commonly employed mean roughness Ra, a new set of surface roughness descriptors for fluid flow character- 'on is presented for fluid flow application in narrow chan- els

## FLOW CONSTRICTION EFFECT ON FRICTION ACTOR

The Moody diagram is simply the Colebrook[4] equat ion over a wide range of Reynolds numbers and relative ess values between 0 and 0.05. The diagram serves as

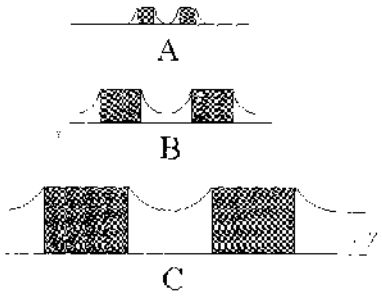


FIG. 1. Degrees of separation of flow from the tube wall over different size elements (sand grain roughness was used by Nikuradse [Ref. 3]). (a). Roughness dominant region; (b) and (c), constriction dominated region.

an easy way to estimate the friction factor without performing a somewhat tedious calculation from the Colebrook equation.

The laminar friction factor, as seen from the Moody's diagram, is independent of the relative roughness in the range 81Drrr 0.05. In the turbulent region, the friction factor for smooth tubes continuously decreases with increasing Reynolds numbers. For rough tubes, the friction factor follows the smooth tube plot up to a certain point, and then approaches an asymptotic value independent of the Reynolds number. The asymptotic value of the friction factor increases with relative roughness in the range 0 <=e/Dl<= 0.05.

In the usage of the Moody diagram, it is assumed that the flow utilizes the entire cross-sectional area defined by the base diameter of the pipe. Following the discussion presented by Webb *et al.*,[6] Fig. I is drawn to show the effects of roughness elements on the reattachment of flow to the pipe walls for different roughness heights. It can be seen from Fig. 1 that for low roughness values, the flow reattaches to the tube wall. At higher roughness values, the flow does not reattach to the pipe wall, thus decreasing the available pipe area for fluid flow. The new flow boundary is suspended above the surface wall at a distance y. The effective diameter of the flow, then, is not the base diameter of the pipe, but is reduced by the size of the roughness elements. While the exact value of this height in comparison to the height of the roughness elements is not known, it is bounded by v=0 and the height of the elements. In closely spaced roughness elements, such as the sand grains used in Nikuradse's' experiments, the value of y closely resembles *c*. The new effective

$$D_a = D_r - 2\varepsilon, \qquad (1)$$

where Da is the constricted flow diameter, D, is the tube (base or root) diameter, and *e* is the average roughness height. Drawing similarity to the compact heat exchanger geometries, it may be noted that the resulting area based on $D_c$r corresponds to the free flow area. On the other hand, following an approach similar to that used in the rarefied gas flow analysis, a slip velocity boundary condition may be introduced after roughness features are properly defined.

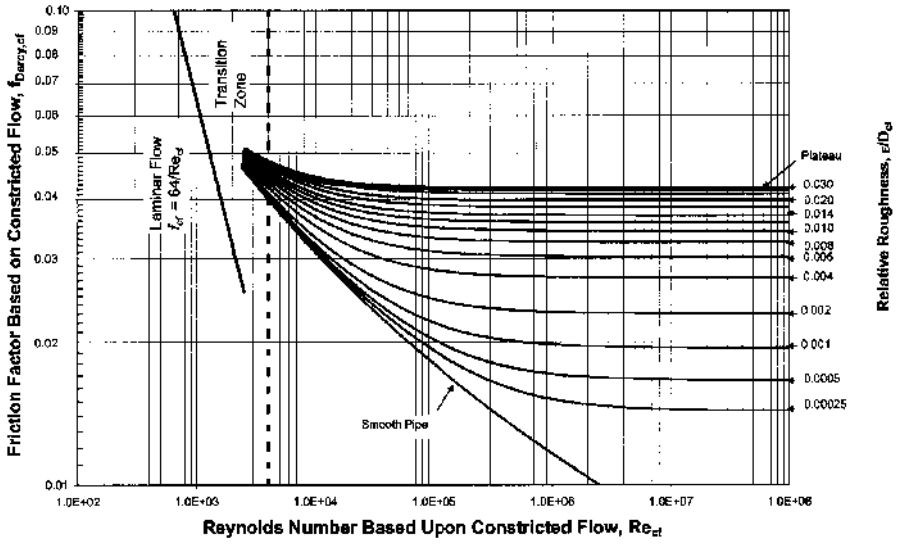


FIG. 2. Darcy friction factor representation based on the constricted flow diameter

In the laminar region, as Webb et 01.[6] pointed out, the roughness height does not seem to affect the flow structure beyond a certain roughness height, as seen from Fig. 1. Therefore the Darcy friction factor based on the constricted flow diameter is expected to be given by substituting the appropriate constricted channel diameter in the friction factor exnressinn!

$$f_{\mathrm{Darcy,cf}} = \frac{64}{\mathrm{Re}_{\mathrm{cf}}}. \tag{2}$$

The subscript cf refers to the constricted flow and $Re_d$ is the Reynolds number based on the constricted flow diameter. In practical applications, the diameter employed by designers is actually based on the actual measurements of the tube inner diameter, which corresponds to the constricted flow diameter. It is not a common practice to add 2 elph to this measurement for obtaining the root diameter, which was used in the Nikuradse's[3] experiments. The experiments reported in this work are used to validate this observation. In the turbulent region, the Colebrook expression is modified by introducing the constriction diameter.

The reduction in the flow area, based on the constricted flow diameter, has a strong effect on the friction factor representation.

The relation between the friction factor from the Moody's diagram, f_darcy and the friction factor based on the constricted flow diameter f is riven by

$$f_{\mathrm{Darcy,cf}} = f_{\mathrm{Darcy}}\left[\frac{(D_t - 2\varepsilon)}{D_t}\right]^5. \tag{3}$$

The Reynolds number is also modified using the constricted flow diameter and is given by

$$\mathrm{Re}_{cf} = \frac{4\dot{m}}{\pi D_{cf}\mu}, \tag{4}$$

where $\dot{m}$ is the mass flow rate, kg/s, and $\mu$ is the dynamic viscosity, N s/m$^2$. The Colebrooke equation for friction factor then becomes

$$\frac{1}{\left(\frac{D_t}{D_t - 2\varepsilon}\right)^{2.5} f_{\mathrm{Darcy,cf}}^{0.5}} = -2.0\ln\left(\frac{\frac{\varepsilon}{D_t}}{3.7} + \frac{2.51}{\mathrm{Re}_{\mathrm{cf}}\left(\frac{D_t}{D_t - 2\varepsilon}\right)^{3.5} f_{\mathrm{Darcy,cf}}^{0.5}}\right). \tag{5}$$

The modified equation for pressure gradient for a circular pipe is thus given by

$$\frac{dP}{dx} = \frac{8\dot{m}^2 f_{\mathrm{Darcy,cf}}}{\pi^2 \rho D_{cf}^5}, \tag{6}$$

where $dP/dx$ is the pressure gradient in the flow direction, N/m$^3$, and $\rho$ is the density of the fluid, kg/m3.

Figure 2 shows the modified Moody diagram replotted using Eqs. (4) and (5). The modified friction factor fdarcy, ef and Reynolds number $Re_d$ are both based on the constricted flow diameter $D_{cf}$. It can be seen from Fig. 2 that the essential features of the Moody diagram are retained, in terms of the linear behavior (on a log-log plot) in the laminar region and the transition region leading to an asymptotic value of F_darcy,efat higher Reynolds number. However, a major change is seen in that the

tained for $E/D$,>0.03 at higher $Re_d$ values, plateaus to approximately f_Da$_{rc}$y,ef=0.042. This implies that the roughness effects on the friction factor are completely accounted for through the area constriction effects incorporated in f_Darcy,ef Intuitively, this makes sense as a higher roughness feature would result in a higher flow constriction. This corresponds to the constriction dominated region where the flow does not reattach to the walls as shown in Fig. 2.

In using the Moody diagram, it is customary to measure the tube inner diameter, which in reality represents *Def* and use it in the pressure drop calculations. Recalling Nikuradse's[3] experiments, the base diameter *Dt* was employed in their pressure drop calculations. Although this error is relatively small for the range of roughness employed in the Moody diagram, it could become significant if the diameter correction is not incorporated while extending the Moody diagram for pipes with higher relative roughness values. The fact that f$_{D}$arc$_{y,ef}$ remains constant at 0.042 in the fully rough turbulent region simplifies the pressure drop calculations. It should be noted that in calculating the pressure drop with the modified Moody diagram given in Fig. 2, the actual constricted flow area should be used as given by Eq. ( 4).

## III. ROUGHNESS EFFECT ON FRICTION FACTOR

The roughness imparted on the internal walls of a flow channel is dependent on the manufacturing process. The sand-grain roughness feature is used extensively in fluid mechanics applications. With smaller channel sizes employed in the microchannels (10 um-200 Kum) and minichannels (200μm-3 mm), the relative roughness $e/D_h$ can be significantly greater than the threshold of 0.05 used in the Moody diagram for a given average roughness *e*. In the following section, three parameters are proposed to characterize the surface roughness effects for higher relative roughness, followed by a description of the experimental work with two specific roughness features, in-line sawtooth and offset sawtooth geometries, and their associated friction factors in the laminar and transition regions with air and water as working fluids. Another aspect that will also be studied is the laminar-to-turbulent transition as a function of the relative roughness.

### Roughness characterization

The pioneering work on characterizing the effect of surface roughness on pressure drop by Nikuradse[3] is the foundation for the Moody diagram that pertains to pipes that have relatively low values of relative surface roughness. The underlying data in this diagram was developed by using sand grains to induce known roughness on the inside surfaces of pipes. Consequently, this diagram is used extensively in predicting friction factors for commercial tubes whose roughness features are not too different from the sand-grain roughness. This work provided the foundations for establishing the effects of relative roughness *e/D* on flow characteristics, but, es the relative roughness becomes large, it becomes important to consider additional roughness features as well.

The initial characterization of surface roughness by

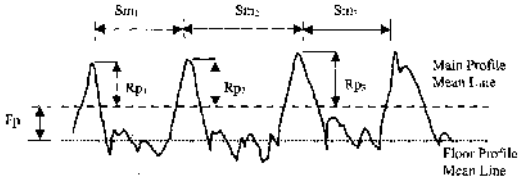


FIG. 3. Maximum profile peak height ($R_p$'s, mean spacing of profile irregularities ($R_{Sm}$), and floor distance to mean line ($F_p$).

(equivalent to the modern descriptor *overage maximum height of the profile, R_z)* and did not consider other parameters that would describe the spacing, waviness, and shape in a three-dimensional area profiling. Additionally, when considering minichannels (3 mm>= $D_B$ > 200 Kum) and micro-channels (200 hem w $D_h$> 10 um) (Kandlikar and Grande), the ratio between the hydraulic diameter and the geometry of the roughness profile becomes significantly different from those in conventional channels. At this scale, the shape, spacing, and size of the roughness irregularities have different influence upon the pressure drop and the overall fluid flow characteristics. In particular, for high values of relative roughness, the flow over roughness features induces recirculation and flow separation and is expected to play a role in single-phase pressure drop. There is clearly a need for developing a set of roughness descriptors suitable for microchannels and minichannels that would allow for a better understanding of the effects of different aspects of surface topography upon the pressure drop and fluid flow behavior.

### *Surface characterization parameters*

In any given channel, the roughness features on the individual channel walls and the resulting variation in the local hydraulic diameter are of interest. A total of three parameters are proposed in the following paragraphs for characterizing the surface roughness feature effect on fluid flow.

Characterizing the individual surfaces. A set of three parameters is proposed to provide information on the roughness features: Maximum profile peak height $R_p$,, mean spacing of profile irregularities Rsm, and the floor distance to mean line $F_p$. Two of these parameters *($R_0$* and Rsm) are defined in the ASME B46.1-2002 (Ref. 10) and the other *(F ,,)* is proposed here. Figure 3 shows these parameters.

( f) Maximum profile peak height *($R_0$):* The distance between the highest point of the profile and the mean line within the evaluation length. The mean line is calculated as Ra (see Fig. 3).

(2) Mean spacing of profile irregularities (Rs.): Consists of the mean value of the spacing between profile irregularities within the evaluation length. The irregularities of interest are

$$R_{Sm} = \frac{1}{n}\sum_{i=1}^{n} Sm_i. \qquad (7)$$

(3) Floor distance to mean line *($F_0$):* Consists of the distance between the main profile mean line (determined by

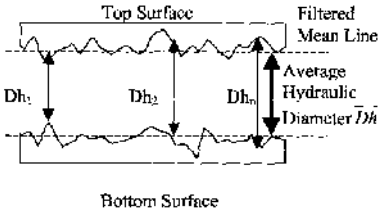


FIG. 4. Variation in the hydraulic diameter along the evaluation length.

$R_5$) and the floor profile mean line. The floor profile is the portion of the main profile that lies below the main profile mean line (see Fig. 3).

The three parameters described above allow for characterization of the peak height, peak spacing, and the distance from the floor to the mean line. These parameters will define the characteristic of the surface roughness that influence the location and shape of the streamlines and, consequently, the size of the recirculation flow zones between roughness elements. From the parameters above, the equivalent roughness s can be estimated by the following relationship:

$$\varepsilon = R_p + F_p. \tag{8}$$

The constricted hydraulic diameter is then estimated by

$$D_{sc} = D_t - 2\varepsilon, \tag{9}$$

where $D_t$ is *the* nominal diameter of the tube, based on the mean floor line.

Characterizing the interaction between the surfaces. Additionally, for example, for a rectangular channel, the opposing surfaces form the channel cross section. The combined effect of the surface features in the effective hydraulic diameter needs to be captured in characterizing the surface roughness. The proposed approach collects the individual profiles and, via digital sampling, calculates the instantaneous hydraulic diameter along the evaluation length of interest for the channel as shown in Fig. 4. The three statistical parameters that need to be collected for characterizing the hydraulic diameter effect are the maximum hydraulic diameter ( Max|D_hi) the minimum hydraulic diameter (MinOwl), and the average hydraulic diameter measured from the filtered mean lines for each surface

$$\bar{D}_h = \frac{1}{n}\sum_{i=1}^{n} |D_{h,i}|. \tag{10}$$

In summary, the following three parameters are proposed to characterize the surface roughness, and three parameters are proposed to characterize the hydraulic diameter for rough channel walls: $R_p$, $Fp$, and Rsm for each individual surface,

Max|D_hi|, Min!D_hi!', and $D\bar{h}$ for the interaction between opposed surfaces. In the experiments conducted in this study, the effect of individual surface roughness features is analyzed and need for further characterization of the hydraulic diameter variation is illustrated. The parameters $R_p$ and $Fp$ are utilized in roughness representation. Other parameters will be incorporated in the future work.

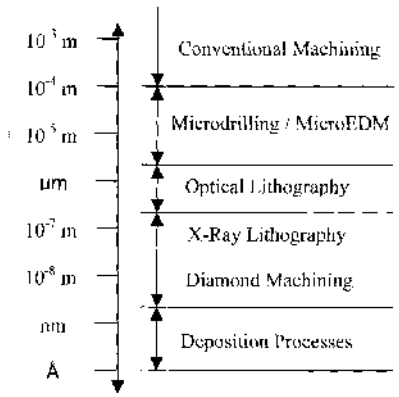


FIG. 5. Dimensional range of micromachining methods.

## IV. SURVEY OF MANUFACTURING PROCESSES

### A. Manufacturing processes and associated surface roughness characteristics

All manufactured products are created with specific materials and geometry to accomplish the function for which they arc intended. The specific geometry of parts can he created via any of the major subsets of processes: phase change, deformation, material addition, or material removal processes. All processes have a direct effect on the surface geometrical properties. The most typical scenario in manufacturing is a balancing act in selecting materials and processes that come together with a proper design to generate the desired product in terms of properties, geometry, and surface characteristics.

Understanding the link between design intent and the performance of a given surface is usually tenuous at best and is most often based on feedback from field experience. Fine surface features are typically described as high frequency variations in the surface, better known as roughness. When a surface is generated on a miniscale or microscale part, the line feature or roughness is typically the only parameter that is relevant because of scale considerations. Figure 5 shows the characteristic surface roughness values for many of the commonly employed manufacturing methods. A brief explanation of the processes relevant to minichannel and microchannel fabrication is included below.

### B. Traditional material removal processes

Machining is the most developed of all processes and very controlled dimensions can be achieved with most materials in use today. Many different methods for material removal have been developed including rotating tool, abrasive, laser, water jet, acid etch, electrical discharge, and other removal processes. All material removal processes work as a type of sculpting process, methodically removing material until the desired part geometry is obtained from a larger starting block. All material removal processes generate the ' gross geometry of the part

features of the surfaces that are generated vary a great deal depending on the material removal method employed. As the feature sizes of the parts are reduced, the relative importance of the surface features is amplified, creating not only a texture, but also the actual features of a size that is relevant on the part surface.

Traditional processes use the rotation of a spindle to generate relative motion between the work part and the tool. The nature of the material removal process is such that the tools will remove material by following paths that overlap to some degree (but not completely) to generate the gross geometry of the part, and as a byproduct, the fine features of the surface. In the minirange microrange, for the same roughness features, the relative roughness is increased significantly because of the small hydraulic diameters.

The past few decades have seen the development of a host of material removal processes that do not make use of a rotating spindle and tool in the traditional manner. Processes that fall under this category include laser machining, water jet cutting, plasma arc cutting, ultrasonic machining, electrical discharge machining (EDM), etc. In EDM, a part surface is eroded via electrical arcing from a tool to the part. The fine surface features of this process, as well as most nontraditional processes are more random in frequency, size, and shape.

### C. Microfabrication processes

Electronics and ever-decreasing feature sizes have had a strong impact on the development of processes to support microfabrication. Layered integrated circuits have caused the development of both material removal and material addition processes in addition to doping processes which change the electrical properties of the parts. This type of process can be very efficient, but the main drawback is poor mechanical material properties. The fine features of microfabricated parts are generated by a series of masking, etching, and deposition processes. Acid/chemical etching and electrically assisted etching techniques are effective in removing material, but great care must be taken to generate the desired geometry by masking or other means. Etching processes are particularly sensitive to crystal structures and grain boundaries that cause variations in the etching rates at different places on the same part. In general etched surfaces take on the features and character of the underlying material structure. The general character of the features can often be exaggerated due to the large number of sequential steps involved, but microfabrication processes are often necessary because there is no other way to accomplish the required design in the production of nicrofabricated parts.

Many of the above processes are employed in manufacturing microchannels and minichannels in diverse applications, including microfluidics, micrometers, high heat flux cooling, biomedical applications, electrokinetically driven flows, etc. The roughness values given in Fig. 5 should be used only as a guideline. Specific flow channel geometries result in surface features that are quite different from those

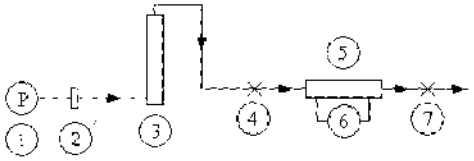


Legend
P - Pressure
1 - Air Supply
2 - Air Filter
3 - Flow Meter
4 - Temperature Sensor
5 - Test Section
6 - Pressure Manifold
7 - Temperature Sensor

FIG. 6. Schematic of the experimental test setup—air.

described in Fig. 5. One such geometry of repeating sawtooth ridges is studied experimentally as described in the following sections.

## V. EXPERIMENTAL VERIFICATION OF THE ROUGHNESS AND FEATURE EFFECTS

The detailed study involving surface roughness feature characterization represents a monumental task, considering the sheer number of configurations that are of interest. In the present work, experimental data are reported for the first time for relative roughness values of up to 0.14. Two roughness features are investigated to bring out the surface feature effect.

The effect of roughness beyond $e/D_h \approx 0.05$ is not studied in literature. In minichannels and microchannels, higher relative roughness may be encountered and the effect of feature size, shape, and distribution on friction factor becomes quite important. To verify this effect, Schmitt" performed an experimental study to evaluate the friction factor for a sawtooth ridged surface in a rectangular minichannel. Two cases were investigated with the ridges *in* the top and bottom channel surfaces either aligned or offset in relation to each other. The details of the experimental setup and the test sections are given by Schmitt and Kandlikar, [12] and some essential features are described below.

Both air and water have been used as test fluids in the present work. Figures 6 and 7 show the respective experimental loops. For the experiments with air, *zero air* is supplied in pressurized cylinders. The air is then passed through a bank of flow meters before entering the test section as shown in Fig. 6. The test section is 100 mm long and has 13 pressure taps located uniformly along its length. The pressure taps are used to identify the location of the fully developed region for obtaining the friction factor data in this region. For experiments with water, de-ionized (DI), degassed water is used as the test fluid. The water is degassed using the procedure described in Kandlikar *et al.*[13] The DI, degassed water is drained into a Fisher Scientific Isotemp 3013 water bath. A positive displacement 1/4 hp bronze gear pump capable of pumping up to 0.9 GPM feeds the test section. A bypass loop is used to control the flow rate through the test section. The water is then filtered using a Shelco FOS

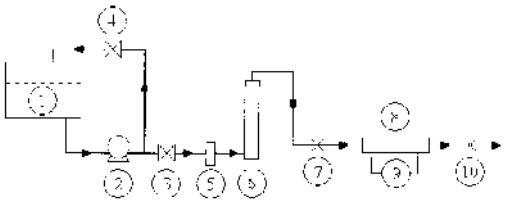

Legend
1. Constant Temperature Water Tank
2. Gear Pump
3. Control Valve
4. By Pass Valve
5. Filter
6. Flow Meter
7. Temperature Sensor
8. Test Fixture
9. Pressure Transducer
10. Temperature Sensor

FIG. 7. Schematic of the experimental test set-up—degassed, DI water.

housing with a 1 *um* wound fiber filter. Three Omega FL5 500-NV rotameter flow meters control the flow rate to the test section.

The pressure taps from the test section are connected to a manifold through valves to facilitate differential pressure measurement, measured from the manifold inlet. Four pressure transducers, with ±6.9 kPa (1 psi), ±34.5 kPa (5 psi), ±103.4 kPa (15 psi), or ±206.8 kPa (30 psi) differential pressure ranges, respectively, are used to cover the entire operating range with air and water. K-type thermocouples measure the fluid temperature before and after the test section. Once the water passes through the test section, it is recirculated into the constant temperature water bath, while the air is discharged into the atmosphere.

## VI. TEST SECTION DETAILS

The test section is made of two individual inserts, each 10.03 mm wide and 100 mm long, forming the top and bottom sides of the flow channel. They are mounted in a fixture that allows the gap between them to be controlled using two micrometers. A photograph of the assembly is shown in Fig. 8. The fluid inlet is through the smooth entrances machined

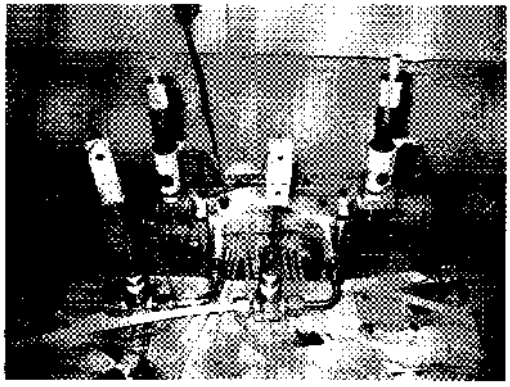

FIG. 8. Photograph of the test section assembly.

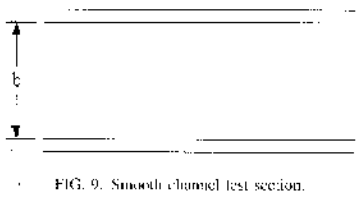


FIG. 9. Smooth channel test section.

on the insets. The surfaces of the insets are machined to provide smooth or rough sawtooth surfaces.

Three surfaces are tested in the current study: (i) smooth, ( ii) aligned sawtooth roughness, and (iii) offset sawtooth roughness. The smooth channel is shown in Fig. 9. The channel is relatively smooth with a maximum average roughness height, $R_z$ of 1.22 ,um. This height is similar to the sand-grain roughness studied by Nikuradse and is therefore used in deriving the constricted flow diameter. The smooth minichannel is used to validate the test section since a smooth channel is expected to follow the conventional flow theory.

The aligned sawtooth roughness arrangement is shown in Hg. 10. It consists of a rectangular minichannel having parallel surfaces with machined ribs running perpendicular to the flow direction. The surface roughness peaks on one side of the channel are lined up to match the surface roughness peaks on the opposite side of the channel.

The offset sawtooth roughness arrangement also consists of parallel surfaces with machined ribs running perpendicular to the flow direction, but the surface roughness peaks are lined up such that the point of one surface roughness peak on one side lies centered between the two surface roughness peaks directly across from it. This is shown in Fig. I1.

The surface roughness parameters were measured using a Mitotoyo SJ-400 profilometer. The results are given in Table I.

## VII. ERROR ANALYSIS

The experimental uncertainty is given as

$$U = \sqrt{B^2 + P_x^2}, \tag{11}$$

where U is the uncertainty, $B$ is the bias error, and is the precision error. Systematic or bias error is generally induced by the error in the measuring instrumentation. Bias can be determined from the least count of the measuring instrumentation. Bias error $B$ is calculated by dividing the accuracy by the target value,

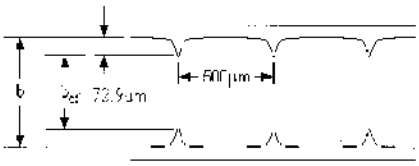


FIG. 10. Aligned sawtooth roughness test section.

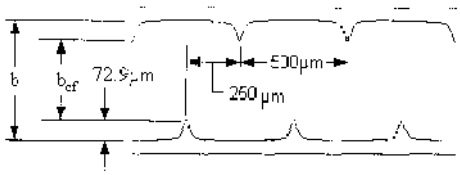


FIG. 11. Offset sawtooth roughness test section.

$$B = \frac{\text{Instrumentation accuracy}}{\text{Measured value}}. \tag{12}$$

Precision error *P* is error induced by a number of measurements. Precision is calculated as

$$P_x = \pm t \times \frac{\sigma_x}{\sqrt{n}}, \tag{13}$$

where *t* is determined from standard *T* tables, is the sample standard deviation, and *n* is the number of samples. Temperature readings arc accurate to ±0.1 °C, air and water flow rates are accurate to ±3% full scale, minichannel dimensions are accurate to ±5 Kum, pressure readings are accurate to ±0.25% full scale, pressure tap distances are accurate to ±5 um and pressure tap locations are accurate to ±5 um. The friction factors were found to have an uncertainty of 8.81%.

## VIII. RESULTS

Tests were conducted for both air and water in minichannels with hydraulic diameters ranging from 325 um to 1819 um, with Reynolds numbers ranging from 200 to 7200 for air and 200 to 5700 for water and the relative roughness values based on the constricted flow diameter ranged between 0. 01 and 0.14. The results for the different test fluids are discussed in the following sections.

### Test section validation

The test section was fitted with smooth inserts and was run with air and water as the working fluids. The experimental results were compared with the theoretical results obtained using the following equations for the Fanning friction factor *f* (*f* =/D,,,/4, as discussed earlier).

Laminar flow. Fanning friction factor,

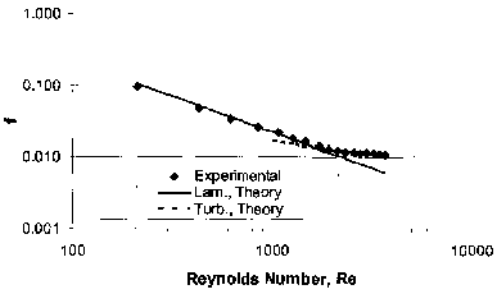


FIG. 12, Fully developed friction factor vs Reynolds number: airflow in smooth channel. $D_h$=953 um,b=500 um w=10.03 min.

$$f = \frac{C}{\mathrm{Re}}, \tag{14}$$

where the constant *C* depends on the aspect ratio of the channel d=b/w, with *b* and w being channel dimensions of a rectangular channel, and is given by the following equation by Kakac *et* a/.[14] (note that *d* ----s- 1, if not replace it with *w/b*):

$$C = 24(1 - 1.3553\alpha^* + 1.9467\alpha^{*2} - 1.7012\alpha^{*3} + 0.9564\alpha^{*4} - 0.2537\alpha^{*5}) \tag{15}$$

In the turbulent region, the Fanning friction factor is given by the following equation (Miller15):

$$f = \frac{0.25\left[\ln\left(\frac{\varepsilon/D_h}{3.7} + \frac{5.74}{\mathrm{Re}^{0.9}}\right)\right]^{-2}}{4}. \tag{16}$$

The applicability of the turbulent friction factor derived for circular tubes to rectangular channels (with the use of hydraulic diameter) was confirmed by Kakac *et* a/.

All pressure drop data along the flow length were analyzed to obtain the fully developed friction factors. This was ascertained by identifying the nonlinear pressure drop in the entry region, followed by the linear region in the fully developed region.

Figures 12 and 13 show a comparison of the experimental results obtained for the smooth channels with the theoretical results obtained from Eq. (14) through (16) for air and water, respectively. The solid line represents the laminar flow and the dotted line represents the turbulent flow. It can be seen that the agreement is quite good, with a mean error of

TABLE I. Minichannel roughness parameters.

| | $R_a$ (μm) | $R_z$ (μm) | $R_{sk}$ | $R_{sv}$ | $R_z$ (μm) | ε (μm) | p/ε |
|---|---|---|---|---|---|---|---|
| Smooth | 0.21 | 0.25 | 0.19 | 3.07 | 1.22 | 0.21 | ··· |
| Aligned | 17.0 | 20.8 | 1.19 | 3.45 | 72.9 | 17.0 | 6.86 |
| Offset | 17.0 | 20.8 | 1.19 | 3.45 | 72.9 | 17.0 | 6.86 |

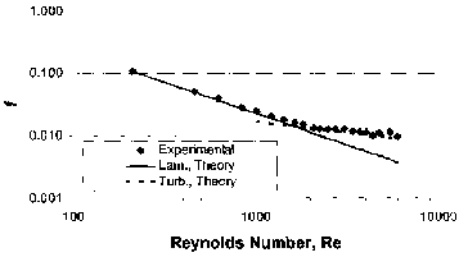


FIG. 13. Fully developed friction factor vs Reynolds number: water flow in smooth channel. $D_h$ = 953 $\mu$m, $b$ = 500 $\mu$m, $w$ = 10.03 mm.

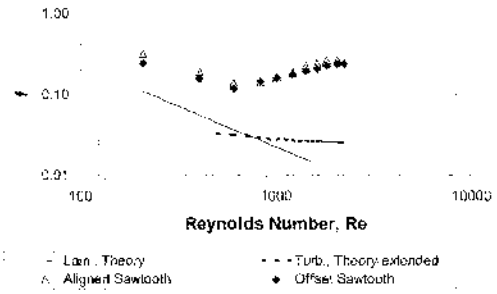


FIG. 15. Fully developed friction factor vs Reynolds number, both based on hydraulic diameter: water flow. $D_h$ = 953 $\mu$m, $b$ = 500 $\mu$m, $b_{ci}$ = 354 $\mu$m, $w$ = 10.03 mm, $e/D_h$ = 0.0735.

less than 3%. Transition from laminar to turbulent flow was observed around Re= 1950. Similar agreement was noted with the water data.

## fx. EFFECT OF ROUGHNESS STRUCTURE

The experiments were conducted with two configurations using insets with sawtooth ridges as shown in Figs. 10 and 11. The gap between the insets was systematically varied to yield different *el Da* ratios. As proposed in Eq. (10), the roughness feature height was used for e, and the hydraulic diameter was calculated using the constricted flow area, with width as w and the constricted gap $b_{ci}$=*6-2e (see* Figs. 10 and 11).

Figures 14 and 15 show the variation of friction factor for the two cases with air and water flow, respectively, using the width and maximum spacing $b$ in calculating the hydraulic diameter (equivalent to the maximum flow cross-sectional area). It is seen that the data do not agree with the theoretical laminar and turbulent cases and lie significantly above the predicted friction factors. It should be noted that the theoretical friction factors are based on the maximum flow area calculated using the root height $h$. The relative roughness $e/D_h$ is 0.0735 for these cases.

Figures 16 and 17 show the same data presented *in* Figs. 14 and 15 for air and water, but the hydraulic diameter and the theoretical friction factors are calculated with the constricted flow area based on $h_e$r. It is seen that the agreement between the experimental data and the respective laminar flow equation is significantly improved (to within less than 5% mean deviation before the transition to turbulent flow). The modified Moody diagram is thus seen to he applicable with the constricted flow area for both sawtooth and aligned roughness features in the laminar flow region.

*In the turbulent* region, the agreement is *quite* poor even with the usage of the constricted flow *area.* The nature of the roughness elements results in a more pronounced difference in some other turbulent test results (>30% in some cases, sec Schmitt' for details). The flow does seem to interact with the base walls even at the high relative roughness values in the transition and turbulent regions. The average roughness value for the sawtooth channels as seen from Table I is Ra =17 um. and the relative roughness value is calculated as 17/953=0.018. Although this is less than 0.05, the conventional Moody plot is not applicable. It clearly points out the need to introduce new parameters to account for the sharp ridges appearing on *the* surface of *the* channel walls. Using the parameters proposed in the earlier section, the mean floor line coincides with the actual channel wall since it is relatively smooth compared to the ridges. Following Eq. (8), the roughness parameter $e$ then corresponds to the height of the ridges, or $e=b$, and the relative roughness is $e/D_{h,rf}$ =0.1108. However, the aligned and offset geometries are still not accurately represented by this parameter, and additional

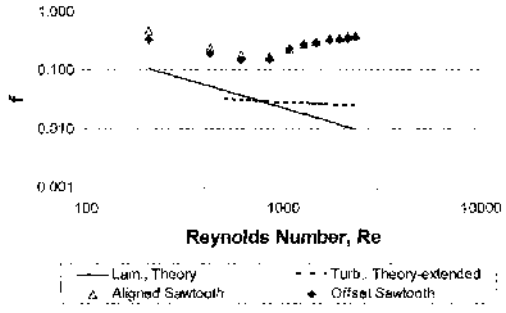


FIG. 14. Fully developed friction factor vs Reynolds number, both based on hydraulic diameter: airflow. $D_h$ = 953 $\mu$m, $b$ = 500 $\mu$m, $b_{ci}$ = 354 $\mu$m, $w$ = 10.03 mm, $e/D_h$ = 0.0735.

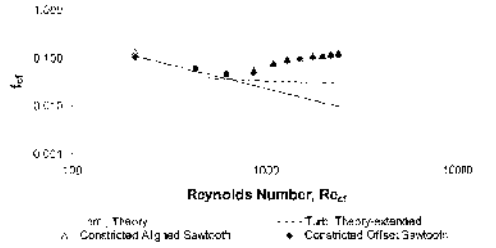


FIG. 16. Fully developed friction factor vs Reynolds number, both based on constricted flow hydraulic diameter: airflow. $D_{h,ci}$ = 684 $\mu$m, $b$ = 500 $\mu$m, $b_{ci}$ = 354 $\mu$m, $w$ = 10.03 mm, $e/D_{h,ci}$ = 0.1108.

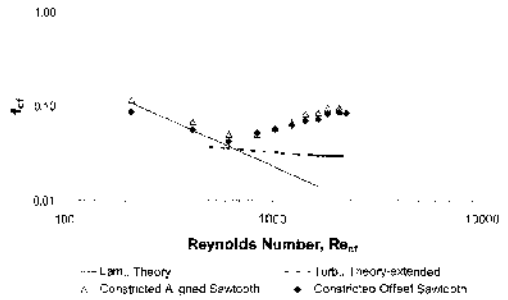


FIG. 17 Fully developed friction factor vs Reynolds number, both based on constricted flow hydraulic diameter: water flow. $D_{h,cf}$=684 $\mu$m, $b$ =500 $\mu$m, $b_{cf}$=354 $\mu$m, $e$=0.03 mm, $e/D_{h,cf}$=0.1108.

considerations, such as using local hydraulic diameter, are warranted. Further work is also needed by varying the sawtooth spacing, ridge heights over the laminar, transition and turbulent regions.

Using the constricted flow diameter, with $E/D\_h$, $ef$ =0.1108, results in significant improvement in the laminar region as seen from Figs. 16 and 17. The theoretical laminar flow friction factor line is calculated using the constricted

$$f_{cf} = \frac{C}{\mathrm{Re}_{cf}}. \qquad (17)$$

The agreement between the theoretical line and the data in the laminar region is quite good. This indicates that the constricted flow diameter clearly governs the flow in the laminar region. The results in the turbulent region are still in significant disagreement. There are also some differences in the performance of the aligned and offset arrangements. Results at other gap spacings are being obtained to compare the aligned and offset structures. A large set of data with different surface features is needed to develop a more specific set of parameters suitable for characterization of roughness effects. Similar results are obtained for different channel heights.

Based on the present work for laminar flow, Eqs. (8) and ( 9) are recommended for determining the surface roughness parameter $e$ and the constricted flow diameter $D_{h,\,f}$ (using b_ef as the constricted gap height in the case of a rectangular channel), and Eq. (17) for the laminar flow friction factor with the constricted flow diameter. The maximum height of the well-defined roughness feature then becomes $s$ for a periodic ridge structure with a relatively smooth floor as used in the present experiments for the aligned and offset saw. tooth geometries. This definition is in agreement with the sand grain roughness value used by Nikuradse. In the turbulent flow region with c /$D_{t}$,.–$_{e}$,f- 0.05, the same roughness parameters described for the laminar flow may be used until more data becomes available showing the effects of roughness features. For higher roughness values beyond $e/DB,,,$ >0.05, and for specific roughness features, there is a need to provide accurate roughness descriptors, such hydraulic diameter. There is also a need to generate more experimental data.

## X. EFFECT OF SURFACE ROUGHNESS ON LAMINAR TO TURBULENT TRANSITION

The transition from laminar to turbulent flow is another area of great interest in microfluidics applications. The current results show that for all gap sizes, the transition to turbulent flow begins at Reynolds numbers in the range 1800-2100 for smooth channels (without any ridges). However, for the sawtooth surface, it is observed that as the relative roughness increases, the transition begins early. For relative roughness values of e/$D_{h}$o=0.06-0.14, the results indicate that the transition Reynolds number based on the constricted flow diameter, Re,,$_{f}$, varies between the values of 800 and 350 for air and water, respectively.

## XI. CONCLUSIONS

(1) The constricted flow area is introduced as an important parameter in representing the effect of roughness on friction factor. A modified Moody diagram is presented with this parameter. The resulting friction factor based on the constricted flow area asymptotically reaches a constant value of $_{fDarcy.cf}$ =0.042 in the fully developed turbulent flow region for 0.03 c/$D_{j}$., -s= 0.05.

(2) The effect of surface roughness features is studied with aligned and offset sawtooth surfaces in a rectangular channel geometry. The height of the sawtooth was used to represent the roughness $e$. The height of the channel was systematically varied to obtain friction data for air and water for e/$D_{)}$,,$_{f}$ of up to 14%.

(3) In the laminar region, the use of the constricted flow hydraulic diameter in the classical laminar flow equation, Eq. ( 17), resulted in a good agreement (within 5%) with the laminar flow data for air as well as water in both aligned and offset sawtooth configurations for 0 $c/D_{cf}$ 0.14.

(4) The laminar-to-turbulent transition is not affected as the channel hydraulic diameter decreases for smooth channels. However, the transition occurs at lower Reynolds numbers ($Re_{cf}$=800 and 350 for 8/$D_{h.cf}$=0.06 and 0.14, respectively) as the relative roughness increases.

(5) In the turbulent region, the experimental friction factors obtained for the two roughness features are considerably above the constant value obtained for $e$ D 0.03 in the modified Moody diagram. Currently there is no predictive method available in the turbulent region beyond e/Dh,cf >0.05. Further, the aligned and offset roughness features resulted in different friction factors in this region. Since the simple roughness parameter $R_{„}$ is unable to correctly describe these surface features, accurate roughness descriptors are needed.

(6) Three parameters are introduced as possible candidates in representing the roughness effect on friction factor in the rough region with $e/D$> 0. Further experimental data and analysis is needed before recommending any specific set to represent the flow effects of surface features.

H. Darcy, *Recherches Experimentales Relatives an Mouvernent de* $Lau$

*dans les Tu,yaux* (Mallet-Bachelier. Paris, France. 1857).

T. Fanning, A *Practical Treatise and Hydraulic and Water Supply Engineering* (Van Nostrand, New York. 1877; revised ed. 1886).

"J. Nikuradse, "Laws of flow in rough pipes" f"Stromungsgesetze in Rauen Rohren," VDI-Farschungsheft 361 11933)]; Reilage nr "Forschung don Gebiele des Ingenieurwesens," Ausgabe B Band 4, English translation NACA Tech. Mem. 1292 (1937).

[O]F. C. Colebrook. "Turbulent flow in pipes. with particular reference to the transition region between the smooth and rough pipe laws," J. Inst. Civ. Eng., Land. 11, 133 (1939).

[5]L. F. Moody, "Friction factors for pipe flow," ASME Trans. J. Appl. Mech. **66,** 671 (1944).

[6]R. Webb, E. R. G. Eckert, and R. J. Goldstein. "Heat transfer and friction in tubes with repeated-rib roughness," Int. J. Heat Mass Transfer 14, 601 (1971).

[v]G. M. Mala and D. Li. "Flow characteristics in microtubes," Mt. J. Heat Fluid Flow 20, 142 (1999).

X. Wang and X. F. Peng, "Experimental investigation on liquid forced convection heat transfer for liquid flowing through microchannel," Int. J. Heal Mass Transfer 30, 73 (1994).

'S. G. Kandlikar and W. J. Grande, "Microchannels and minichannels History. terminology, classification and current research needs," First International Conference on Microchannels and Minichannels. Rochester, New York, 24-25 April 2003.

'ASME Standard B46.1-2002. *Surface Texture (Surface Roughness, Wariness, and Lay ), The American Society* $_{Q}$*t Mechanical Engineers, An Amerima Napional Spandard (20021,* pp. 1-98.

D. J. Schmitt, "Experimental investigation of surface roughness microstructures and their effects on pressure drop characteristics in rectangular minichannels," M.S. thesis. Department of Mechanical Engineering. Rochester Institute of Technology, 2004.

'[2]D. J. Schmitt and S. G. Kandlikar. "Effects of repeating microstructures on pressure in rectangular minichannels," Third International Conference on Microchannels and Minichannels, Toronto, Canada, 13-15 June 2004. ASME Paper No. ICNIM20051 I.

"[3]S. G. Kandlikar, M. E. Steinke, and P. Balasubramanian, "Single-phase flow characteristics and effect of dissolved gases on heat transfer near saturation conditions in microchannels," Proceedings of IMECE02, New Orleans, LA, November 2002.

"S. Kakac, R. K. Shah, and W. Aung, *Handbook of Single-Phase Convective Heat Transfer (Wiley,* New York, 1987), pp. 3 122.

[I:6]R. W. Miller, *Flow Measuremenp Engineering Handbook,* 3rd ed. ( McGraw-1E11, New York, 1996).